



Article

# Water Contaminated by Industrial Textile Dye: Study on Decolorization Process

Pierantonio De Luca <sup>1,\*</sup>, Paola Foglia <sup>2</sup>, Carlo Siciliano <sup>3</sup>, János B. Nagy <sup>2</sup> and Anastasia Macario <sup>2,\*</sup>

<sup>1</sup> Dipartimento di Ingegneria Meccanica, Energetica e Gestionale. Università della Calabria, I-87036 Arcavacata di Rende (CS), Italy

<sup>2</sup> Dipartimento di Ingegneria per l'Ambiente ed il Territorio ed Ingegneria Chimica. Università della Calabria, I-87036 Arcavacata di Rende (CS), Italy

<sup>3</sup> Dipartimento di Farmacia e Scienze della Salute e della Nutrizione. Università della Calabria, I-87036 Arcavacata di Rende (CS), Italy

\* Correspondence: pierantonio.deluca@unical.it (P.D.L.); anastasia.macario@unical.it (A.M.); Tel.: +39-09-8449-6757 (P.D.L.); +39-09-8449-6704 (A.M.)

Received: 25 July 2019; Accepted: 26 August 2019; Published: 2 September 2019



**Abstract:** This work aims to investigate possible interferences due to the presence of sodium carbonate on the photodegradation of the reactive Black 5 azoic dye, both in systems containing only titanium oxide and those containing titanium oxide and hydrogen peroxide. The role of hydrogen peroxide is explicitly treated. Sodium carbonate, in fact, is often present in the wastewater of textile industries as it is used in the fiber dyeing phases. The use of TiO<sub>2</sub> nanoparticles is emphasized, and the possible danger is underlined. Each system was subjected to ultraviolet irradiation (UV) by varying the exposure time. After the photodegrading tests, the resulting solutions were analyzed by UV-vis spectrophotometry and High-Resolution Nuclear Magnetic Resonance to measure the residual concentrations of dye. The dye degradation curves and reaction rates for different UV exposure times were obtained and discussed as a function of the used additives. All the data are repeated three times, and they differ only by a maximum of 5%. The results indicated a reduction of about 50% of the initial concentration of Reactive Black 5 after 30 min under optimal experimental conditions. The NMR analysis indicated the formation of a series of aromatic structures that were generated by the UV-induced photochemical fragmentation of the original molecule.

**Keywords:** reactive black-5; azo-dye; photodegradation; sodium carbonate; titanium dioxide; hydrogen peroxide

## 1. Introduction

There are already many polluting substances that put the environment and human health at risk [1–6]. In order to improve the environmental conditions, many researchers have carried out numerous studies for the development of innovative materials that respect the environment [7–11].

Alongside the development of new materials, particular interests have been turned to the study of eco-friendly processes designed to purify the wastewater using sunlight, a renewable and clean energy. In this “pro environment” context, the photochemistry is having a great development through the application of photocatalysis, a natural phenomenon that is manifested by a chemical reaction that mimics the photosynthesis of plants to absorb and transform pollutants into harmless elements [12–17] in the presence of specific substances called photocatalysts. In this sense, in-depth studies conducted in recent years have shown that among the substances that can act as photocatalysts, the semiconductor oxides are the most efficient results in the promotion of the transformation reactions of the pollutants

in the presence of light. Particularly appreciated for its excellent photocatalytic action is the titanium dioxide, especially in its crystallographic form of anatase [18–20]. Recently, however, one has tried to widen the range of substances that may be used as photocatalysts, and among the new species there are the zeolitic materials [21–29], and adsorption materials such as microporous materials and carbon nanotubes [30–36].

The use of nanoparticle TiO<sub>2</sub> (average size of 15 nm) is inherently a dangerous process due to environmental release [37]. Many studies highlight nanoparticle emission due to nanocoatings [38] and tiles [39,40]. Cases of nanoparticle exposure in the field of occupational hygiene in workplaces have been reported [41]. Knowing the large use of these nanoparticles [42] and the risk of the release of these types of products in the environment [43,44], one has to emphasize the exposure risk to the consumer [45]. These aspects are also addressed in relation to metrological challenges related to particle characterization [46]. In particular, textile and paper industries produce wastewater with high concentrations of harmful dyes that are very difficult to degrade. In fact, the efficiency of the fixation of dyes is between 60% and 90%, and approximately 1–20% of the dye production is lost during the staining process and released in wastewater. Thus, the development of effective approaches for the treatment of industrial wastewater containing pollutants is a challenge for the protection of the environment and human health. Azo dyes themselves have a minor environmental effect because they make effluent streams highly colored. However, their precursors and degradation products, such as aromatic amines, can cause dermal and respiratory diseases, allergies, skin and mucous membrane irritation, and carcinogenesis [47,48]. In general, reactive azo dyes are degraded and removed from the aqueous environment by processes that are photocatalytic-based, and sonication-induced degradation treatments [49]. Zeolites [50–55] have been proposed as effective dye adsorbents. Immobilization techniques of reactive azo dyes on alkyl calixarene materials have also been studied [56–58]. In this context, synthetic calixarene-based resins were found to be excellent [59]. Absorption by cellulose and synthetic polymeric materials, microgels, magnetic amine/metal oxide functionalized biopolymer resins, and anaerobic/aerobic membrane reactors have recently been investigated [60–63]. Photoelectrochemical treatments by an iron mesh double layer such as an anode, electrocoagulation using sacrificial iron electrodes, or metal plates activated with carbon materials, have been proven to be efficient auxiliary methods for the remediation of azo dye polluted waters [64–66]. Sawdust, coal-based activated carbon, carbon char, and simple or functionalized multi-walled carbon nanotubes (MWCNTs) have been proposed as adsorbents [67,68]. Among the available nanomaterials, cellulose nanocrystals-reinforced keratin bioadsorbents, zero-valent nano-copper, protein nanofibrils, and the loading of Ag/AgCl nanoparticles, have been proposed for the remediation of wastewater. These methods allow for the coagulation and/or homogeneous and heterogeneous oxidation of textile azo dyes through the Fenton reaction, which can also be carried out on nanotube arrays [69].

However, the limitations in using conventional methods for the treatment of dyes are the high resistance of dyes to biodegradation, the high water-solubility of these aromatic compounds, and their poor adsorption capabilities onto the sludge. Hence, most of these methods offer a lower efficiency for degradation. As an alternative, studies on the applicability of naturally available adsorbents from agricultural and industry waste materials, fruit and plant waste, and natural inorganic material as bio-adsorbents have recently been reviewed [70]. Among these systems, surfactant modified barley straw, sun flower seed shells, rice agricultural waste microbes, bacterial strains, crude enzymes, marine microorganisms and yeasts, and  $\beta$ -cyclodextrins synergically combined with metal oxides, have been used for the aerobic decolorizing and biological degradation of azo dyes [71]. However, the efficiency of these eco-friendly adsorption methods showed a high dependence on the pH of the medium in the treatment process. In general, all reported studies have proven that the treatment of textile dyeing wastewater by various combinations of biological methods might be inadequate. Traditional methods mainly provide a phase transfer of the contaminants from wastewater to the sludge. Alternatively, advanced oxidation processes are promising technologies that aim at the decolorizing and mineralization of a wide range of azo dyes into stable inorganic compounds, or,

at least, their transformation into biodegradable and harmless products. Many studies have been carried out for the design of innovative and eco-friendly processes and technologies based on the use of sunlight as a renewable and clean UV source to repair waters [72]. In these approaches, semiconductor oxides have been found to be the most efficient photocatalysts in the transformation of azo dyes in the presence of light. The potential of photocatalysis by  $\text{TiO}_2$  for the removal of dyes from aqueous solutions has been widely studied [73], and heterogeneous systems based on the use of  $\text{TiO}_2$  nanoparticles supported on different materials in the presence of UV irradiation have attracted interest due to their efficiency [74,75]. However, low quantum yields limit the practical application of titanium dioxide photocatalytic processes. The photonic efficiency in the decolorization of azo dyes can be improved by using eco-friendly redox additives, such as peroxydisulfate or  $\text{H}_2\text{O}_2$  under UV irradiation. These systems have been investigated with the aim of supplementing the low photonic efficiency of conventional UV photocatalysis in the presence of  $\text{TiO}_2$ , and the efficiency of these photooxidation techniques have clearly been highlighted [76–82], although possible interferences on the photodegradation of the azo dye, by salts such as sodium carbonate, have been little investigated. It is known that effluents of textile dyeing industries contain significant amounts of inorganic salts, such as chlorides and carbonates [83,84]. Inorganic anions occur naturally in wastewater or may be added to facilitate the dyeing process [85]. Thus, the presence of inorganic anions might play an important role in the photooxidation kinetics of different azo dyes.

The research in the field of treatment of waste water produced by textile industries is challenging. Today, the exploitation of bio-sustainable and chemical bio-compatible methods for the remediation of waters containing azo dyes needs new impulses. This study is focused on the photooxidation of Reactive Black 5, an azo dye that is commonly used in the textile industry. The process was carried out under UV irradiation, in the presence of  $\text{TiO}_2$  and the redox additive  $\text{H}_2\text{O}_2$ , in an aqueous solution containing  $\text{Na}_2\text{CO}_3$ . The main objective of the present work was to investigate, by ultraviolet irradiation (UV) laboratory-scale experiments, the influence of the additive  $\text{H}_2\text{O}_2$  and the inorganic salt  $\text{Na}_2\text{CO}_3$  on the catalytic activity of  $\text{TiO}_2$  during the decolorization of Reactive Black 5 azo dye. The peroxide additive  $\text{H}_2\text{O}_2$  has been studied with the aim to improve the photodegradation process. The basic salt sodium carbonate was used to investigate whether its presence might produce effects in the photodegradation of Reactive Black 5. Experiments were performed by simulating the composition of wastewater produced from the textile industry, which employs  $\text{Na}_2\text{CO}_3$  in the tissue color fixing process. The novelty of the present work consists in the investigation of the Reactive Black 5 degradation, when this dye is treated with well-known economic and environmentally friendly methods that can be modified by the presence of basic salts in waste water generated by the industrial color fixing process. Being aware that the photocatalytic system  $\text{TiO}_2/\text{H}_2\text{O}_2/\text{UV}$ -light has been widely experimented on, the use of inorganic salts as cheap, smart, and chemically bio-compatible partners of the above cited system has only seldom been reported and investigated.

## 2. Materials and Methods

The azo-dye Reactive Black-5 (Sigma-Aldrich, Darmstadt, Germany) (Figure 1, empirical formula  $\text{C}_{26}\text{H}_{21}\text{N}_5\text{Na}_4\text{O}_{19}\text{S}_6$ , molecular weight 991.82) was used in all experiments.

Titanium dioxide ( $\text{TiO}_2$ ) (Anatase- 99.6% Alfa Aesar, Karlsruhe, Germany) was used as the photocatalytic agent (15 nm average particle size, surface area  $50 \text{ m}^2/\text{g}$ ), together with hydrogen peroxide (30% (w/w), Sigma-Aldrich, Germany) and the basic inorganic salt sodium carbonate (Sigma-Aldrich, Darmstadt, Germany). All systems were irradiated with a UV lamp (100 W,  $\lambda = 365 \text{ nm}$ ). The intensity of irradiation was low ( $1 \text{ mW}/\text{cm}^2$ ), because a recombination of electron-hole pairs is occurring at higher intensity [86]. The concentration of 30% w/w is chosen for  $\text{H}_2\text{O}_2$  solution, because an excess can have a detrimental effect acting as a scavenger of Valence Band holes and  $^\circ\text{OH}$ , producing hydroperoxide radicals  $\text{HO}_2^\circ$  that have a less oxidizing power than  $^\circ\text{OH}$  [86].

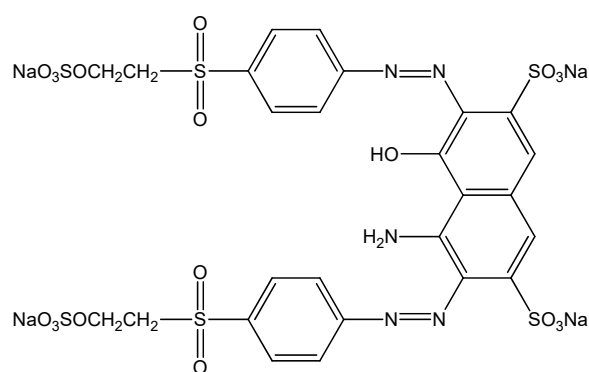


**Figure 1.** Molecular structure of Reactive Black-5.

At the end of the photocatalytic tests, the resulting solutions were filtered by microfilters (0.45  $\mu\text{m}$ ) and analyzed by UV-VIS spectrophotometry (UV-3100 PC-VWR), in order to measure the residual concentrations of dye as observable after photodegradation. All experiments were performed in triplicate, and the results were reported as the mean values. All graphics report the mean values obtained for all measurements. A significant standard deviation less/equal to 5% was determined for all runs (not reported in the figures in order to avoid embedding).

High-Resolution Nuclear Magnetic Resonance analysis (HR-NMR) methods used for the structural determination of organic compounds in complex mixtures [87,88] were also applied on samples of the starting water solutions and the resulting solutions obtained from the photodegrading process, in order to assess the efficiency of the UV treatment. NMR experiments were performed with a Bruker Advance AC300 instrument, by fixing the probe temperature at 25  $^{\circ}\text{C}$ . Samples (480  $\mu\text{L}$ ) of the aqueous solutions were spiked with a small amount of DMSO- $d_6$  (20  $\mu\text{L}$ ) as the spectral calibrating agent. All chemical shifts were reported in ppm and referenced to the signal of residual DMSO protons (2.50 ppm). The spectra were recorded as previously reported [89,90].

The isotherm curves and reaction rates were analyzed for different UV exposure times and discussed as a function of the additives used. Initially, an aqueous solution of Reactive Black-5 dye was prepared with a 0.003% weight-to-weight concentration, and the same solution was used to prepare different systems that were subsequently subjected to photodegradation under UV irradiation, during different times (Table 1).

**Table 1.** Composition of the initial systems subjected to a photocatalytic test; Concentrations of the dye solution = 30 mg/L;  $\text{H}_2\text{O}_2$  solution = 30% (*w/w*).

System	Composition
0	10 mL dye solution
1	10 mL dye solution + 0.01 g $\text{TiO}_2$
2	10 mL dye solution + (0.01 g $\text{TiO}_2$ + 0.01 g $\text{Na}_2\text{CO}_3$ )
3	10 mL dye solution + 0.5 mL $\text{H}_2\text{O}_2$
4	10 mL dye solution + (0.01 g $\text{TiO}_2$ + 0.5 mL $\text{H}_2\text{O}_2$ )
5	10 mL dye solution + (0.01 g $\text{TiO}_2$ + 0.5 mL $\text{H}_2\text{O}_2$ + 0.01 g $\text{Na}_2\text{CO}_3$ )

Initially, the azo-dye photostability was investigated either in the absence or in the presence of titanium dioxide, without adding other reagents.

Further tests were carried out on the same systems containing  $\text{TiO}_2$ , after adding other additives such as sodium carbonate (determining in all cases a salt concentration of sodium carbonate equal to 1 g/L) and hydrogen peroxide. This was made in order to study and improve the photocatalytic activity of titanium dioxide. Each system was prepared by adding the required amounts of components in a batch reactor, operating at atmospheric pressure. The following order was applied for reactants: dye

solution, titanium oxide, hydrogen peroxide, and sodium carbonate. The systems were stirred at room temperature for two minutes.

Subsequently, all aqueous systems were irradiated with a UV lamp for different times under magnetic stirring. Table 1 reports the compositions of all of the studied systems.

### 3. Results and Discussion

#### 3.1. UV Analysis

The results were plotted to have a clear vision of the residual concentration of dye after the UV irradiation, and the variation of pH. The plots obtained for all systems are shown below, together with the system coloring.

##### 3.1.1. System 0 (10 mL of Dye Solution)

This system, containing only the dye and no photocatalytic agent, was initially tested to study the natural photocatalytic stability of the dye (Figure 2). UV irradiation alone was not sufficient to degrade the dye in suitable times. In fact, after 7 h of irradiation, the dye was degraded only to a 10% extent. This proves the very limited tendency of the dye to photodegradation, at least in the absence of added photocatalytic agents. The pH value remained close to neutrality, and no color variations of the aqueous system were observed (Figure 3), confirming the evidence for the photocatalytic resistance of the dye.

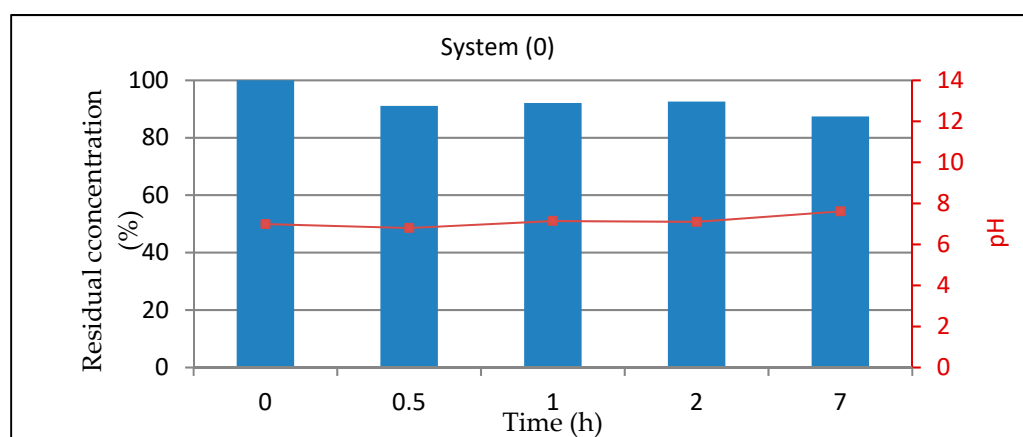


**Figure 2.** Residual concentration (%) and pH for System 0, as a function of the UV irradiation time exposure.

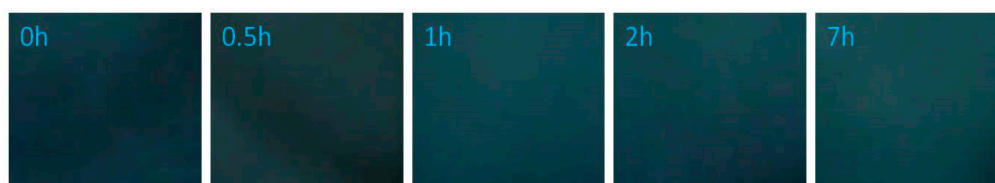


**Figure 3.** Variation of the color solution for System 0, as a function of the UV irradiation time exposure.

##### 3.1.2. System 1 (10 mL of Dye Solution/0.01 g TiO<sub>2</sub>)

The results obtained using TiO<sub>2</sub> as the photocatalyst are reported in Figure 4.

In the presence of TiO<sub>2</sub>, a significant dye photodegradation was observed. After 2 h of UV irradiation, the extent of dye photodegradation was at almost 80%. The UV irradiated aqueous solution showed an evident discoloration (Figure 5). As already observed for System 0, the pH value did not change significantly.

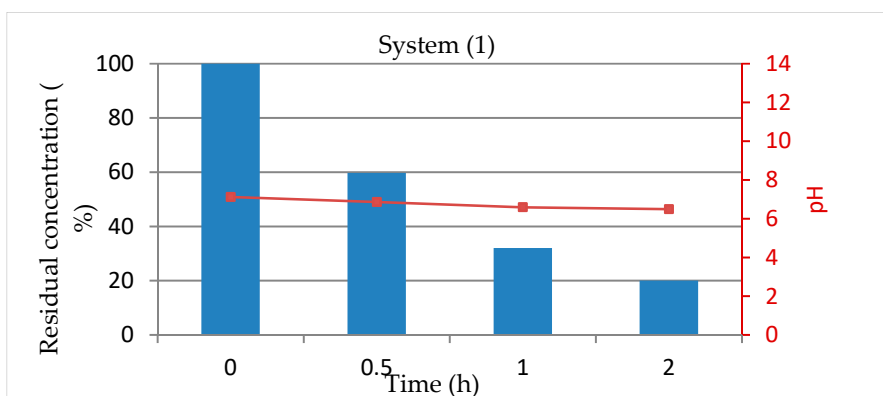


**Figure 4.** Residual concentration (%) and pH for System 1, as a function of the UV irradiation time exposure.

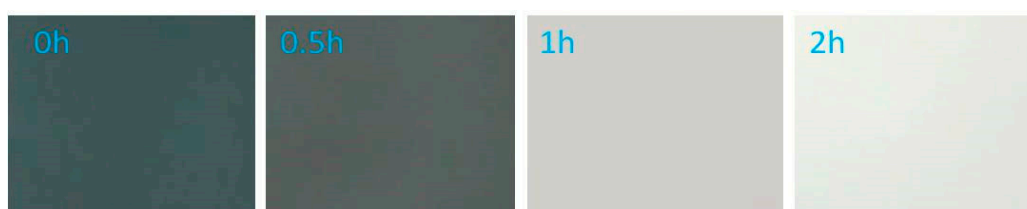


**Figure 5.** Variation of the color solution for System 1, as a function of the UV irradiation time exposure.

### 3.1.3. System 2 (10 mL Dye Solution + (0.01 g TiO<sub>2</sub> + 0.01 g Na<sub>2</sub>CO<sub>3</sub>))

The study of this system, containing sodium carbonate, was undertaken taking into account that the basic inorganic salt is generally used to fix the color on the textiles, since it induces a pH increase. In fact, it is important for the dye molecules to fix up with the fiber during the industrial manufacturing process. Therefore, it was reputed interesting to test any variation of the photoactivity of titanium dioxide by simulating aqueous environments containing Reactive Black-5 and sodium carbonate.

The collected data (Figure 6), showed that the activity of titanium dioxide was not affected by the presence of sodium carbonate. In fact, the photodegradation activities of Systems 1 (TiO<sub>2</sub> only) and 2 (TiO<sub>2</sub> and Na<sub>2</sub>CO<sub>3</sub>) were found to be similar. In this case, the pH value increased due to the presence of sodium carbonate. Although the color of the basic solution was affected by the presence of Na<sub>2</sub>CO<sub>3</sub>, the discoloration trend after the UV irradiation was comparable to that shown by the system containing only TiO<sub>2</sub> (Figure 7).

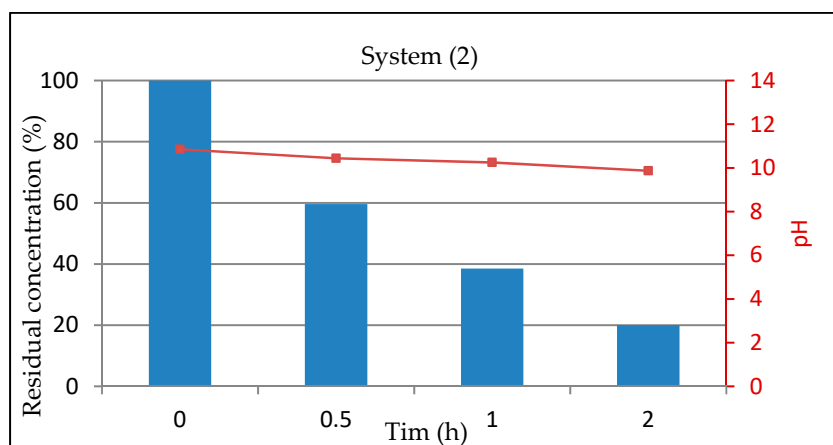


**Figure 6.** Residual concentration (%) and pH for System 2, as a function of the UV irradiation time exposure.

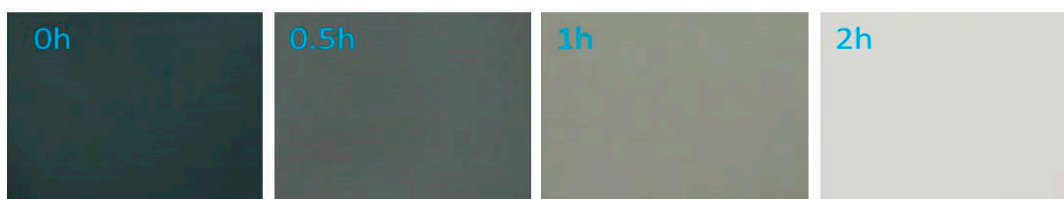


**Figure 7.** Variation of the color solution for System 2, as a function of the UV irradiation time exposure.

#### 3.1.4. System 3 (10 mL Dye Solution + 0.5mL H<sub>2</sub>O<sub>2</sub>)

System 3 contained H<sub>2</sub>O<sub>2</sub>, and no TiO<sub>2</sub> and Na<sub>2</sub>CO<sub>3</sub> were added. This system was tested in order to investigate the effect of the peroxide on the dye photodegradation. The system was maintained under UV irradiation for 2 h, and after this time the dye photodegradation was limited to 20% (Figure 8). Although no evident changes in color were observed (Figure 9), the use of hydrogen peroxide was not satisfactory for obtaining an appreciable diminution of the dye. The presence of hydrogen peroxide maintained the solution pH at 4.

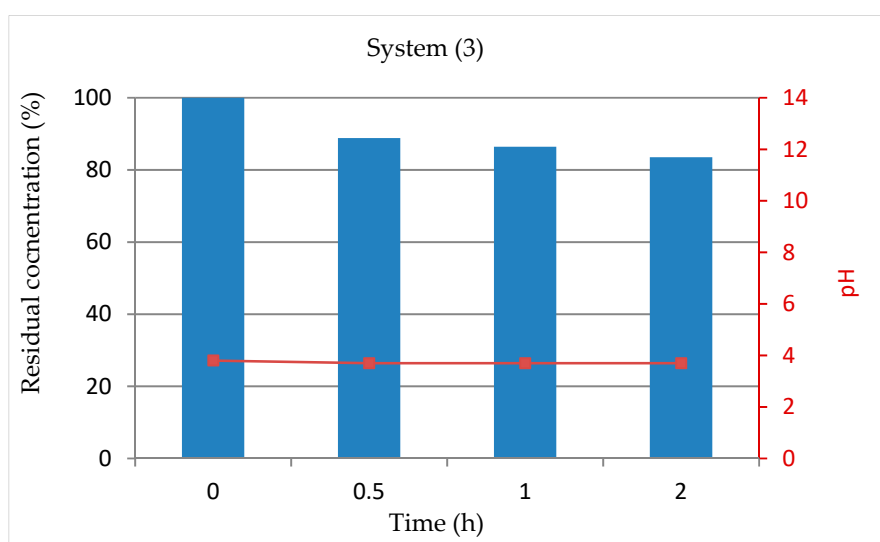


**Figure 8.** Residual concentration (%) and pH for System 3, as a function of the UV irradiation time exposure.



**Figure 9.** Variation of color for System 3, as a function of the UV irradiation time exposure.

#### 3.1.5. System 4 (10 mL Dye Solution + (0.01 g TiO<sub>2</sub> + 0.5mL H<sub>2</sub>O<sub>2</sub>))

The addition of titanium oxide to the solution of System 3 determined a gradual decreasing of the dye concentration (Figure 10).

These results were compared to those reported in Figure 4 for System 1, containing only TiO<sub>2</sub> as a photocatalyst. In this case, an increased activity of titanium dioxide was registered, since the solution showed an evident decolorizing after only 30 min (0.5 h) of irradiation (Figure 11), while the pH value did not show appreciable variations (Figure 10).

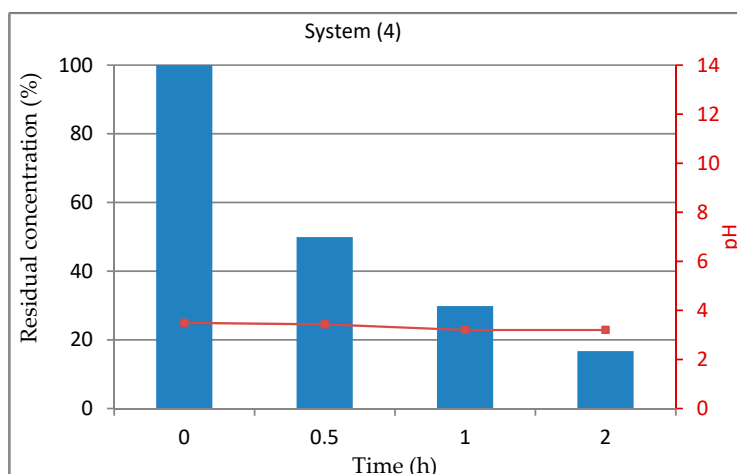


**Figure 10.** Residual concentration (%) and pH for System 4, as a function of the UV irradiation time exposure.

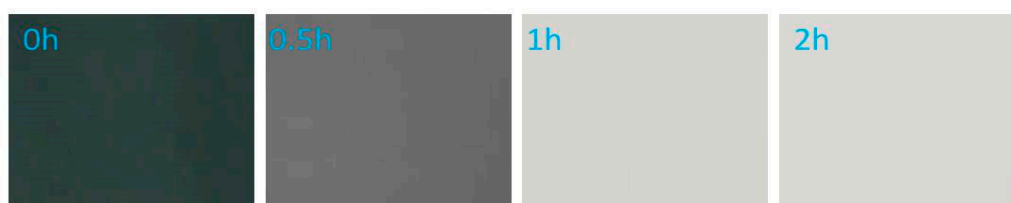


**Figure 11.** Variation of the color solution for System 4, as a function of the UV irradiation time exposure.

$\text{H}_2\text{O}_2$  is an oxidant species that positively influences the photocatalytic reaction, due to the formation of hydroxyl radicals  $^{\circ}\text{OH}$ . The production of  $^{\circ}\text{OH}$  radicals could be written as:  $\text{TiO}_2\text{-H}_2\text{O}_2 \rightarrow \text{TiO}_2\text{-}^{\circ}\text{OH} + ^{\circ}\text{OH}$  [86].

The decolorizing, caused by the low concentration of the solution that still retains 30% of dye, was obtained after 1 h, and prolonged times of treatment were useless. As in the study case, the fully decolorized water solution obtained after 1 h of UV exposure was subjected to a high resolution  $^1\text{H}$  NMR analysis, in order to evaluate the dye photoconversion extent. An aliquot of the water residue was placed in the NMR, and the calibrating agent was added. The recorded spectrum (Figure 12) showed a high complexity for the regions of aromatic and methylene protons.

The signal set appearing between 7.60 and 8.20 ppm, associated with the resonances of aromatic protons, indicated the formation of a series of aromatic structures that were generated by the UV-induced photochemical fragmentation of the original molecule. The photochemical diazotization of the dye produced a further set of not well resolved signals in the range between 3.00 and 5.50 ppm, due to the formation of a series of compounds characterized by differently substituted short polar alkyl chains. All these signals were strongly overlapped by the water proton signals at 4.50 ppm. In general, a complete recognition of all polar compounds arising from the photochemical disruption of bonds sensible to UV irradiation could be performed by applying an in situ chemical functionalization together with a suitable instrumental analysis and theoretical data treatments [91–94]. In this case, all polar compounds originating from the dye photo-induced dissociation are water soluble; thus, the pre-analysis chemical functionalization of the sample could be unsatisfactory, due to the possible non-complete recovery of products that are formed in low concentrations, and to the unwanted hydrolysis of functionalizing reagents. As a consequence, NMR spectroscopy only gave information about the qualitative composition of the samples, and no other specific data related to the structure of any single compound were obtained. NMR was used as a qualitative method in order to establish any possible change of the resonances attributable to the residual dyes in the solutions, and to detect newly formed degradation products coming from the decolorizing process.



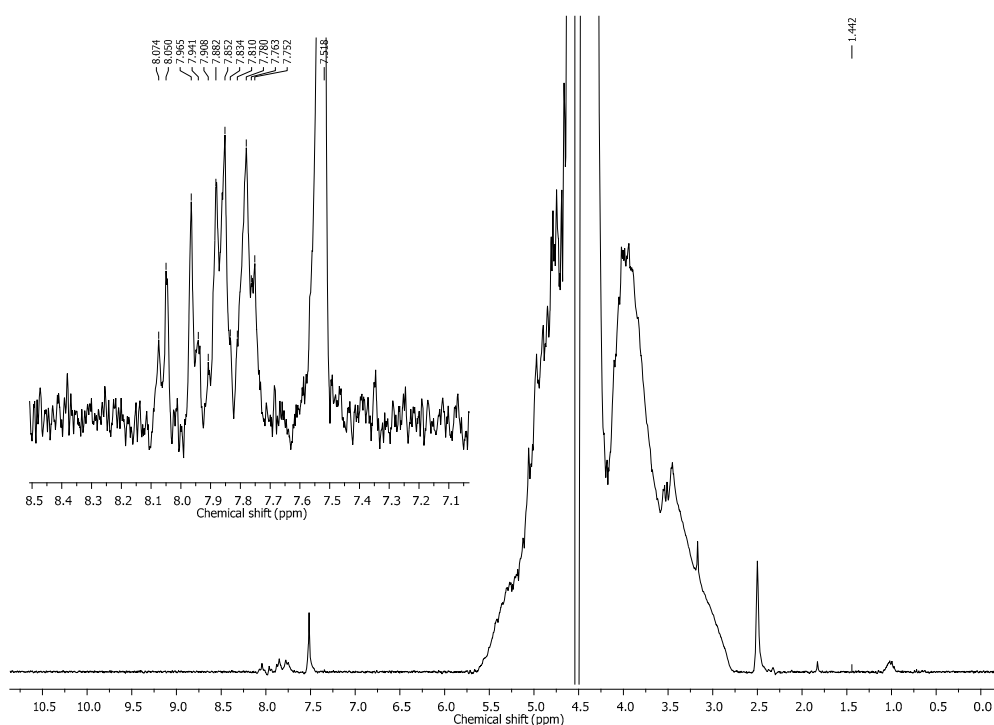


**Figure 12.** <sup>1</sup>H NMR spectrum recorded for a sample obtained from the experiment performed with System 4.

3.1.6. System 5 (10 mL Dye Solution + (0.01 g TiO<sub>2</sub> + 0.5mL H<sub>2</sub>O<sub>2</sub> + 0.01 g Na<sub>2</sub>CO<sub>3</sub>)

System 5 was prepared by adding sodium carbonate to System 4. The basic inorganic salt was used in order to evaluate its influence in water environments where titanium dioxide and hydrogen peroxide could simultaneously be present.

The results reported in Figure 13 show that sodium carbonate did not affect the photodegradation process in the presence of TiO<sub>2</sub> and H<sub>2</sub>O<sub>2</sub>. An increase of the turbidity and pH value of the solution was observed, as expected due to the presence of sodium carbonate (Figure 14).

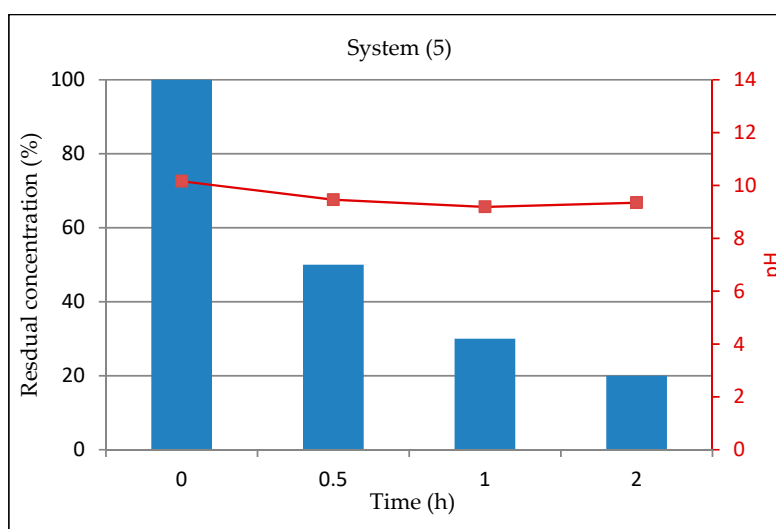


**Figure 13.** Residual concentration (%) and pH for System 5, as a function of the UV irradiation time exposure.

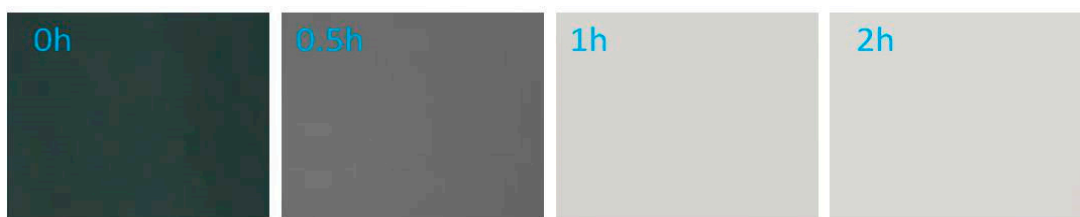


Figure 14. Variation of the color solution for System 5, as a function of the UV irradiation time exposure.

### 3.2. Comparison between Systems

The data plotted in Figures 15–18 report the amount of degraded dye/amount of titanium dioxide ratios, as a function of the UV time exposure. In particular, each figure compares this relation between the analyzed systems. The scope is to study the role played by additives, hydrogen peroxide and sodium carbonate, on the titanium dioxide activity in the reactive black-5 photodegradability.

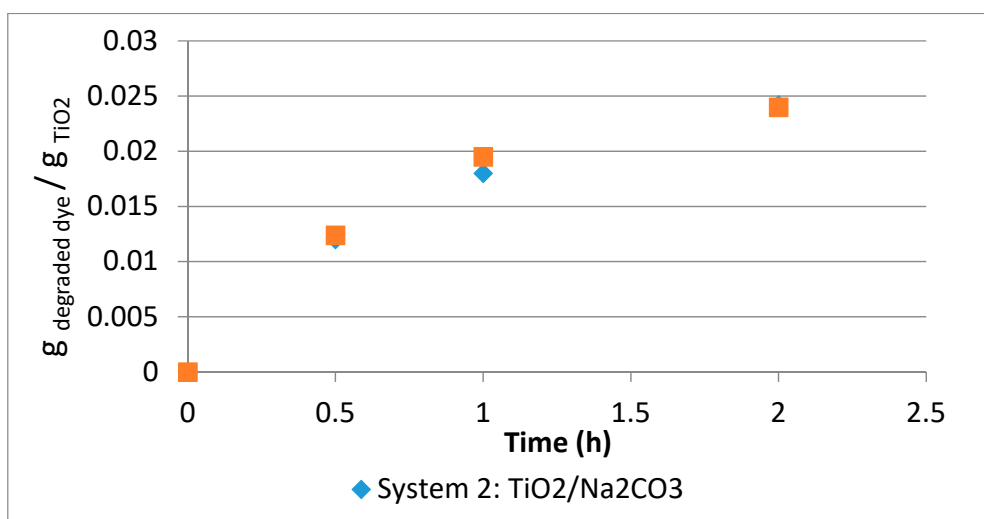


Figure 15. Comparison of the dye degradation curves for Systems 1 and 2.

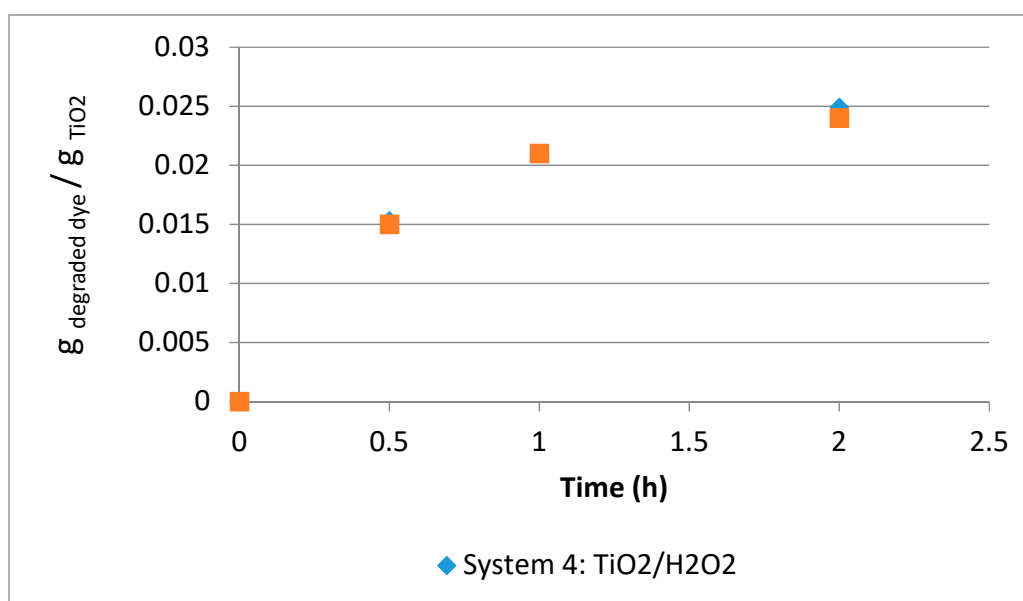


Figure 16. Comparison of the dye degradation curves for Systems 4 and 5.

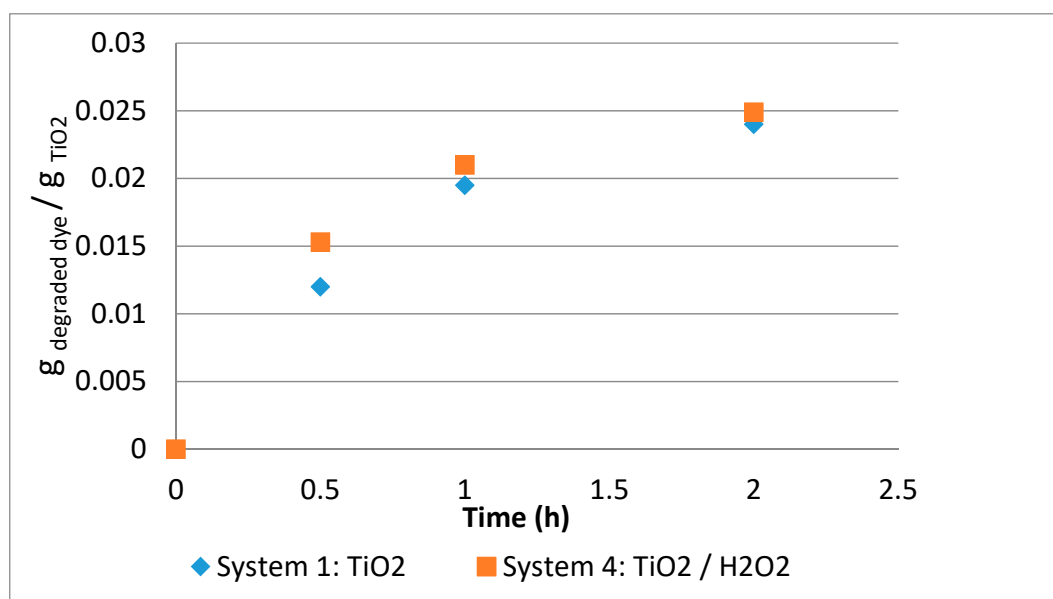


Figure 17. Comparison of the dye degradation curves for Systems 1 and 4.

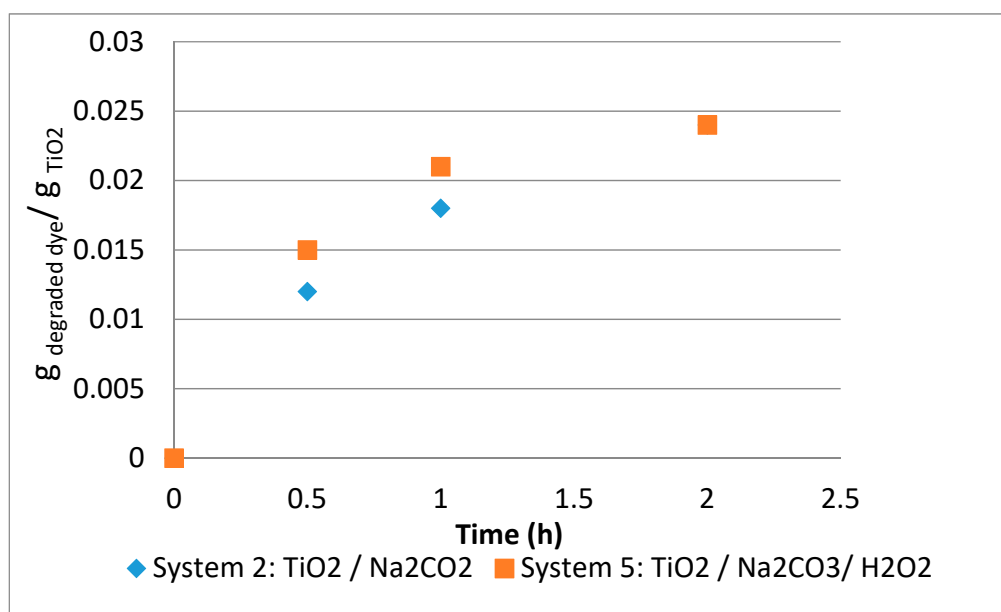
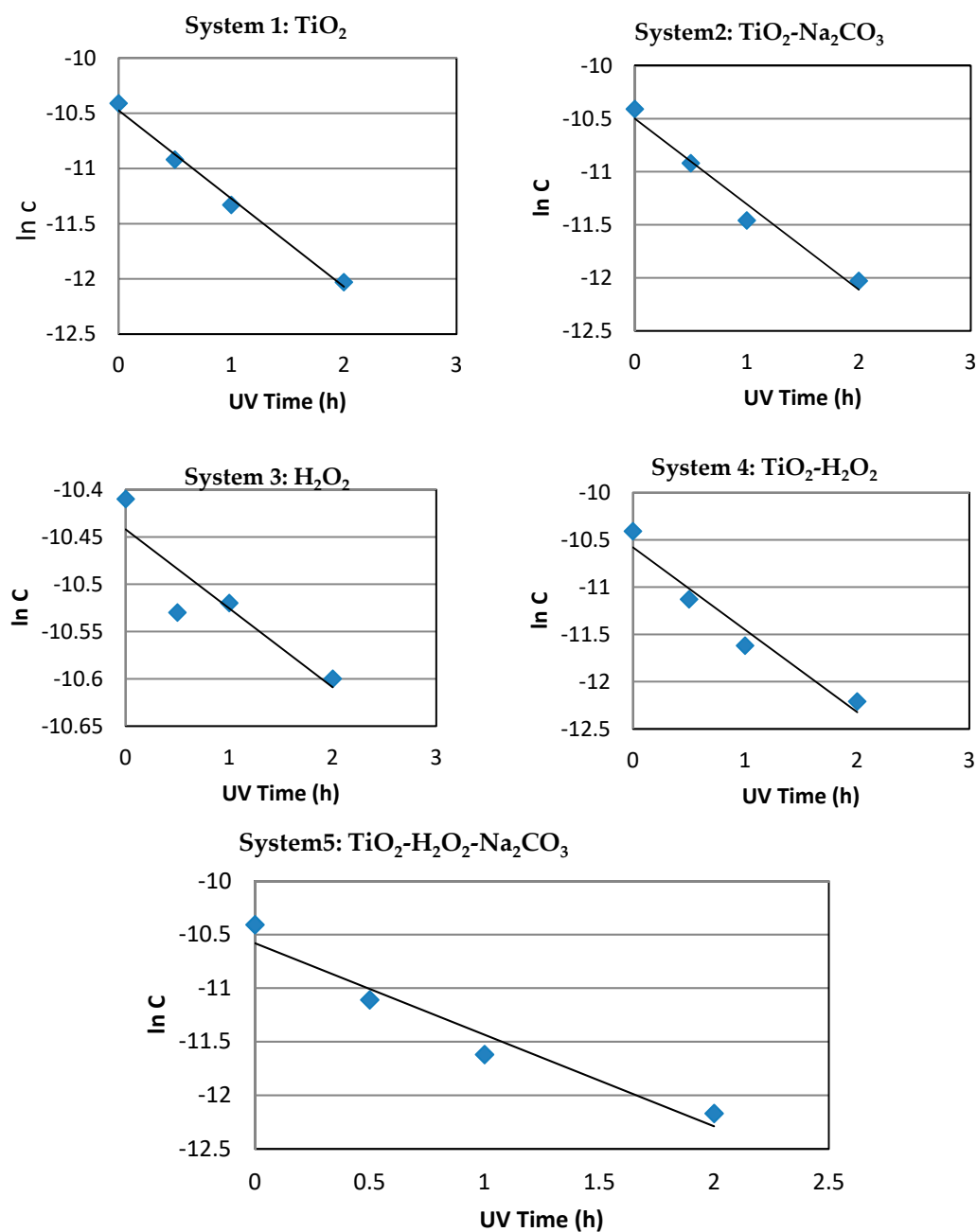


Figure 18. Comparison between the dye degradation curves for Systems 2 and 5.

Figures 15 and 16 compare systems that differ only in presence or absence of sodium carbonate. It can be observed that sodium carbonate does not make a clear improvement in photodegradation, but can be considered as an inert agent, and in fact the curves are almost overlapping. Instead, Figures 17 and 18 below compare systems that differ only in the presence or absence of hydrogen peroxide.

This comparison confirmed that the presence of hydrogen peroxide, in all systems where titanium dioxide was added, accelerated the dye photodegradation process. The observed trend was most noticeable in the interval between 0.5 and 1 h of UV exposure. Finally, the reactivity of the two systems did not show modifications after two hours of irradiation. The graphs reported in Figure 19 show the change of residual molar concentrations of the dye on a logarithmic scale as a function of the UV exposure time. The kinetic results obtained for all Systems 1–5 are reported in Table 2.



**Figure 19.** Residual molar concentrations of the dye versus the UV irradiation exposure time (logarithmic scale).

**Table 2.** Kinetic results for Systems 1–5.

	Additives	K (h <sup>-1</sup> )	ln C	R <sup>2</sup>
System 1	TiO <sub>2</sub>	0.80	10.5	0.992
System 2	TiO <sub>2</sub> -Na <sub>2</sub> CO <sub>3</sub>	0.81	10.5	0.973
System 3	H <sub>2</sub> O <sub>2</sub>	0.08	10.4	0.823
System 4	TiO <sub>2</sub> -H <sub>2</sub> O <sub>2</sub>	0.87	10.6	0.952
System 5	TiO <sub>2</sub> -H <sub>2</sub> O <sub>2</sub> -Na <sub>2</sub> CO <sub>3</sub>	0.85	10.6	0.948

Except for System 3, which was subjected to a photodegradation process assisted only by H<sub>2</sub>O<sub>2</sub>, all other Systems' study cases can be carefully described by a first order kinetics. For Systems 1 and 2, the kinetic parameters were found to be similar, which means that the presence of sodium carbonate

did not modify the reactivity. Systems 4 and 5 showed an increased reactivity with respect to Systems 1 and 2 due to the presence of  $H_2O_2$ . The rate constant increase ranged from 6 to 9%. The rate constant of System 3 was ten times smaller than that observed for all other Systems, although the reaction cannot appropriately be described by applying a pseudo-first order rate model.

#### 4. Conclusions

From the set of results obtained, it is clear that the Reactive Black 5 azo dye in the absence of photocatalytic agents is fairly photostable; in fact, after thirty minutes of UV radiation, a reduction of only 8.9% is recorded. Even in the presence of hydrogen peroxide only, the dye does not change its photostability much, which is around 11.2% after thirty minutes of UV radiation. Titanium oxide instead plays a fundamental role in the UV-induced photodegradation of Reactive Black 5 azo dye, and the photocatalytic activity of titanium dioxide can be improved through the simultaneous use of hydrogen peroxide. The use of only hydrogen peroxide is not sufficient for the complete dye photodegradation, although the presence of peroxides improved the photoactivity of titanium dioxide.

The photocatalytic process with titanium dioxide could be limited by the fast recombination of electron-hole pairs, and the addition of hydrogen peroxide to water systems promoted the dye photodegradation. The hydrogen peroxide, in fact, is used to increase the amount of hydroxyl radicals, which are responsible for the UV-induced degradation. Comparing the system with only titanium oxide and the system with titanium oxide and hydrogen peroxide after thirty minutes of UV irradiation, the percentage reduction of dye is respectively 40.3% and 50.1%, therefore with an improvement of about 10% with respect to the system with only titanium oxide.

Adding sodium carbonate to water systems does not exert a significant impact on the photodegradation of the dye. In this case, only an increase of the solution's turbidity is observed. The observed decolorizing of water solutions containing the Reactive Black 5 dye is mainly due to the photo-induced cleavage of the azo bond in its structure, affording several differently hydroxylated by-products. In all experiments, it can be supposed that dye molecules are oxidized by hydroxyl radicals generated by the  $TiO_2$ -assisted photocatalytic process in the presence of  $H_2O_2$  as an additive under UV irradiation [95,96]. This process is also pH-sensitive, and the mechanism has already been reported [97]. As a consequence, the photo-degradation mechanism was not further investigated. Although the photo-degradation was not performed on acidic pH values, the basic conditions adopted for the set of experiments, in order to simulate the textile industry dye fixing process, highlighted that the action of the system  $TiO_2/H_2O_2/CO_3^{2-}$  was not accelerated when compared with the same process performed in the absence of the basic salt. By considering the anionic form of the Reactive Black 5 dye at a basic pH, the formation of an excess of anionic charges on the photocatalyst surface was supposed to be responsible for the kinetics observed in the case of water samples that did not contain the inorganic salt. This evidence was finally supported by the literature data [97].

Moreover, the time of the UV exposure can play a fundamental role. In fact, a more prolonged UV irradiation increases the percentage of dye photodegradation. Therefore, this method can be proposed for the elimination of other dyes used in the industry. Moreover, it could be coupled with the use of adsorbents (zeolites, carbon nanotubes) in order to recover the dyes one could use for further applications.

**Author Contributions:** Conceptualization, P.D.L.; Data curation, P.F.; Formal analysis, C.S., P.F.; Methodology, P.D.L., C.S.; Supervision, P.D.L., A.M. and J.B.N.; Writing—original draft, P.D.L.

**Funding:** This research received no external funding.

**Conflicts of Interest:** The authors declare no conflict of interest.

#### References

1. Di Filippo, P.; Pomata, D.; Riccardi, C.; Buiarelli, F.; Gallo, V. Oxygenated polycyclic aromatic hydrocarbons in size-segregated urban aerosol. *J. Aerosol. Sci.* **2015**, *87*, 126–134. [[CrossRef](#)]

2. Zhuo, S.; Du, W.; Shen, G.; Li, B.; Liu, J.; Cheng, H.; Xing, B.; Tao, S. Estimating relative contributions of primary and secondary sources of ambient nitrated and oxygenated polycyclic aromatic hydrocarbons. *Atmos. Environ.* **2017**, *159*, 126–134. [[CrossRef](#)]
3. Filice, M.; De Luca, P.; Guido, G.P. Particular matter pollution in university area: Traffic flow analysis. *Environ. Eng. Manag. J.* **2009**, *8*, 1407–1412. [[CrossRef](#)]
4. Livesley, S.J.; McPherson, E.G.; Calfapietra, C. The Urban Forest and Ecosystem Services: Impacts on Urban Water, Heat, and Pollution Cycles at the Tree, Street, and City Scale. *J. Environ. Qual.* **2016**, *45*, 119–124. [[CrossRef](#)] [[PubMed](#)]
5. Squillace, P.J.; Scott, J.C.; Moran, M.J.; Nolan, B.T.; Kolpin, D.W. VOCs, Pesticides, Nitrate, and Their Mixtures in Groundwater Used for Drinking Water in the United States. *Environ. Sci. Technol.* **2002**, *36*, 1923–1930. [[CrossRef](#)] [[PubMed](#)]
6. Wei, B.; Yang, L. A review of heavy metal contaminations in urban soils, urban road dusts and agricultural soils from China. *Microchem. J.* **2010**, *94*, 99–107. [[CrossRef](#)]
7. Venkatarama Reddy, B.V. Sustainable materials for low carbon buildings. *Int. J. Low Carbon Technol.* **2009**, *4*, 175–181. [[CrossRef](#)]
8. Guigo, N.; Mija, A.; Vincent, L.; Sbirrazzuoli, N. Eco-friendly composite resins based on renewable biomass resources: Polyfurfuryl alcohol/lignin thermosets. *Eur. Polym. J.* **2010**, *46*, 1016–1023. [[CrossRef](#)]
9. De Luca, P.; Roberto, B.; Vuono, D.; Siciliano, C.; Nagy, J.B. Preparation and optimization of natural glues based on larice pine resin. *Iop Conf. Ser. Mater. Sci. Eng.* **2018**, *374*, 012071. [[CrossRef](#)]
10. Mohanty, A.K.; Misra, M.; Drzal, L.T. Sustainable Bio-Composites from Renewable Resources: Opportunities and Challenges in the Green Materials World. *J. Polym. Environ.* **2002**, *10*, 19–26. [[CrossRef](#)]
11. De Luca, P.; Carbone, I.; Nagy, J.B. Green building materials: A review of state of the art studies of innovative materials. *J. Green Build.* **2017**, *12*, 141–161. [[CrossRef](#)]
12. Petronella, F.; Truppi, A.; Ingrosso, C.; Placido, T.; Striccoli, M.; Curri, M.L.; Agostiano, A.; Comparelli, R. Nanocomposite materials for photocatalytic degradation of pollutants. *Catal. Today* **2017**, *281*, 85–100. [[CrossRef](#)]
13. Yang, X.; Qin, J.; Jiang, Y.; Chen, K.; Yan, X.; Zhang, D.; Li, R.; Tang, H. Fabrication of P25/Ag<sub>3</sub>PO<sub>4</sub>/graphene oxide heterostructures for enhanced solar photocatalytic degradation of organic pollutants and bacteria. *Appl. Catal. B Environ.* **2015**, *166–167*, 231–240. [[CrossRef](#)]
14. Chen, J.; Poon, C. Photocatalytic Cementitious Materials: Influence of the Microstructure of Cement Paste on Photocatalytic Pollution Degradation. *Environ. Sci. Technol.* **2009**, *43*, 8948–8952. [[CrossRef](#)] [[PubMed](#)]
15. Poon, C.S.; Cheung, E. NO removal efficiency of photocatalytic paving blocks prepared with recycled materials. *Constr. Build Mater.* **2007**, *21*, 1746–1753. [[CrossRef](#)]
16. Serpione, N.; Pellizzatti, E. *Photocatalysis Fundamental and Applications*; Sons, J.W., Ed.; Wiley: New York, NY, USA, 1989.
17. De Luca, P.; De Luca, P.; Candamano, S.; Macario, A.; Crea, F.; Nagy, J.B. Preparation and characterization of plasters with photodegradative action. *Buildings* **2018**, *8*, 122. [[CrossRef](#)]
18. Chiing-Chang, C.; Fu-Der, M.; Kung-Tung, C.; Chia-Wei, W.; Chung-Shin, L. Photocatalyzed N-de-methylation and degradation of crystal violet in titania dispersions under UV irradiation. *Dye. Pigm.* **2007**, *75*, 434–442.
19. Fujishima, A.; Rao, T.N.; Tryk, D.A. Titanium dioxide photocatalysis. *J. Photochem. Photobiol. Photochem. Rev.* **2000**, *1*, 1–21. [[CrossRef](#)]
20. Macounová, K.; Urban, J.; Krýsová, H.; Krýsa, J.; Jirkovský, J.; Ludvík, J. Photodegradation of metamitron(4-amino-6-phenyl-3-methyl-1,2,4-triazin-5(4H)-one) on TiO<sub>2</sub>. *J. Photochem. Photobiol. A Chem.* **2001**, *140*, 93–98.
21. D’Auria, M.; Emanuele, L.; Racioppi, R.; Velluzzi, V. Photochemical degradation of crude oil: Comparison between direct irradiation, photocatalysis, and photocatalysis on zeolite. *J. Hazard. Mater.* **2009**, *164*, 32–38. [[CrossRef](#)]
22. Manouchehr, N.; Khodayar, G.; Kazem, M. Photocatalytic degradation of azo dye Acid Red 114 in water with TiO<sub>2</sub> supported on clinoptilolite as a catalyst. *Desalination* **2008**, *219*, 293–300.
23. Uma, S.; Rodrigues, S.; Martyanov, I.N.; Klabunde, K.J. Exploration of photocatalytic activities of titanosilicate ETS-10 and transition metal incorporated ETS-10. *Micropor. Mesopor. Mat.* **2004**, *67*, 181–187. [[CrossRef](#)]
24. De Luca, P.; Chiodo, A.; Nagy, J.B. Activated ceramic materials with deposition of photocatalytic titano-silicate micro-crystal. *Sustain. Chem.* **2011**, *154*, 155–165.

25. Nash, M.; Lobo, R.F.; Doren, D.J. Photocatalytic oxidation of ethylene by ammonium exchanged ETS-10 and AM-6. *Appl. Catal. B-Environ.* **2009**, *88*, 232–239. [[CrossRef](#)]
26. Vuono, D.; Guzzo, M.; De Luca, P.; Nagy, J.B. Physico-chemical characterization of zirconium-based self-bonded ETS-4 pellets. *J. Therm. Anal. Calorim.* **2014**, *116*, 169–182. [[CrossRef](#)]
27. Guoqing, G.; Tetuya, K.; Katsuki, K.; Kunio, K.; Eiichi, A.; Akira, Y. Photocatalytic reactivity of noble metal-loaded ETS-4 zeolites. *Inorg. Chem. Commun.* **2004**, *7*, 618–620.
28. Turta, N.A.; De Luca, P.; Bilba, N.; Nagy, J.B. Synthesis of titanosilicate ETS-10 in presence of cetyltrimethylammonium bromide. *Microporous Mesoporous Mater.* **2008**, *112*, 425–431. [[CrossRef](#)]
29. De Luca, P.; Mastroianni, C.; Nagy, J.B. Synthesis of self-bonded pellets of ETS-4 phase by new methodology of preparation. *IOP Conf. Ser. Mater. Sci. Eng.* **2018**, *347*, 012003. [[CrossRef](#)]
30. De Luca, P.; Vuono, D.; Filice, M. Self-bonded ETS-10 pellets containing iron. *Environ. Eng. Manag. J.* **2009**, *8*, 1009–1015. [[CrossRef](#)]
31. De Luca, P.; Poulsen, T.G.; Salituro, A.; Tedeschi, A.; Vuono, D.; Könya, Z.; Madarász, D.; Nagy, J.B. Evaluation and comparison of the ammonia adsorption capacity of titanosilicates ETS-4 and ETS-10 and aluminotitanosilicates ETAS-4 and ETAS-10. *J. Therm. Anal. Calorim.* **2015**, *122*, 1257–1267. [[CrossRef](#)]
32. De Raffe, G.; Aloise, A.; De Luca, P.; Vuono, D.; Tagarelli, A.; Nagy, J.B. Kinetic and thermodynamic effects during the adsorption of heavy metals on ETS-4 and ETS-10 microporous materials. *J. Porous Mater.* **2016**, *23*, 400. [[CrossRef](#)]
33. Wang, S.; Peng, Y. Natural zeolites as effective adsorbents in water and wastewater treatment. *Chem. Eng. J.* **2010**, *156*, 11–24. [[CrossRef](#)]
34. De Luca, P.; Bernaudo, I.; Elliani, R.; Tagarelli, A.; Nagy, J.B.; Macario, A. Industrial Waste Treatment by ETS-10 Ion Exchanger Material. *Materials* **2018**, *11*, 2316. [[CrossRef](#)] [[PubMed](#)]
35. Policicchio, A.; Vuono, D.; Rugiero, T.; De Luca, P.; Nagy, J.B. Study of MWCNTs adsorption performances in gas processes. *J. CO<sub>2</sub> Util* **2015**, *10*, 30–39. [[CrossRef](#)]
36. De Luca, P.; Nappo, G.; Siciliano, C.; Nagy, J.B. The role of carbon nanotubes and cobalt in the synthesis of pellets of titanium silicates. *J. Porous Mater.* **2018**, *25*, 283–296. [[CrossRef](#)]
37. Warheit, D.B. Hazard and risk assessment strategies for nanoparticle exposures: How far have we come in the past 10 years? *F1000Research* **2018**, *7*, 376. [[CrossRef](#)]
38. Morgener, M.; Aguerre-Chariol, O.; Bressot, C. Stem imaging to characterize nanoparticle emissions and help to design nanosafe paints. *Chem. Eng. Res. Des.* **2018**, *136*, 663–674. [[CrossRef](#)]
39. Bressot, C.; Aubry, A.; Pagnoux, C.; Aguerre-Chariol, O.; Morgener, M. Assessment of functional nanomaterials in medical applications: Can time mend public and occupational health risks related to the products' fate? *J. Toxicol. Environ. Healthpart A* **2018**, *81*, 957–973. [[CrossRef](#)]
40. Bressot, C.; Manier, N.; Pagnoux, C.; Aguerre-Chariol, O.; Morgener, M. Environmental release of engineered nanomaterials from commercial tiles under standardized abrasion conditions. *J. Hazard. Mater.* **2017**, *322*, 276–283. [[CrossRef](#)]
41. Bressot, C.; Shandilya, N.; Jayabalan, T.; Fayet, G.; Voetz, M.; Meunier, L.; Le Bihan, O.; Aguerre-Chariol, O.; Morgener, M. Exposure assessment of nanomaterials at production sites by a short time sampling (sts) approach strategy and first results of measurement campaigns. *Process Saf. Environ. Prot.* **2018**, *116*, 324–332. [[CrossRef](#)]
42. Piccinno, F.; Gottschalk, F.; Seeger, S.; Nowack, B. Industrial production quantities and uses of ten engineered nanomaterials in Europe and the world. *J. Nanopart. Res.* **2012**, *14*, 1–11. [[CrossRef](#)]
43. Keller, A.A.; Lazareva, A. Predicted releases of engineered nanomaterials: From global to regional to local. *Environ. Sci. Technol. Lett.* **2013**, *1*, 65–70. [[CrossRef](#)]
44. Keller, A.A.; Vosti, W.; Wang, H.; Lazareva, A. Release of engineered nanomaterials from personal care products throughout their life cycle. *J. Nanopart. Res.* **2014**, *16*, 2489. [[CrossRef](#)]
45. Göhler, D.; Stintz, M. Granulometric characterization of airborne particulate release during spray application of nanoparticle-doped coatings. *J. Nanopart. Res.* **2014**, *16*, 1–15. [[CrossRef](#)] [[PubMed](#)]
46. Morgener, M.; Ramirez, A.; Smith, S.M.; Tweedie, R.; Heng, J.; Maass, S.; Bressot, C. Particle technology as a uniform discipline? Towards a holistic approach to particles, their creation, characterisation, handling and processing! *Chem. Eng. Res. Des.* **2019**, *146*, 162–165. [[CrossRef](#)]
47. Hildenbrand, S.; Schmahl, F.W.; Wodarz, R.; Dartsch, P.C. Azo Dyes and Carcinogenic Aromatic Amines in Cell Cultures. *Int. Arch. Occup. Environ. Health.* **1999**, *72*, 11. [[CrossRef](#)]

48. Neumann, H.G. Aromatic Amines in Experimental Cancer Research: Tissue-Specific Effects, an Old Problem and New Solutions. *J. Crit. Rev. Toxicol.* **2007**, *37*, 211–236. [[CrossRef](#)]
49. Eren, Z. Ultrasound as a basic and auxiliary process for dye remediation: A review. *J. Environ. Manag.* **2012**, *104*, 127–141. [[CrossRef](#)]
50. Benkli, Y.E.; Can, M.F.; Turan, M.; Çelik, M.S. Modification of organo-zeolite surface for the removal of reactive azo dyes in fixed-bed reactors. *Water Res.* **2005**, *39*, 487–493. [[CrossRef](#)]
51. Alver, E.; Metin, A.U. Anionic dye removal from aqueous solutions using modified zeolite: Adsorption kinetics and isotherm studies. *Chem. Eng. J.* **2012**, *200–202*, 59–67. [[CrossRef](#)]
52. Armağan, B. Factors affecting the performances of sepiolite and zeolite for the treatment of textile wastewater. *J. Environ. Sci. Health A* **2003**, *38*, 883–896. [[CrossRef](#)]
53. Armağan, B.; Ozdemir, O.; Turan, M.; Celik, M.S. The removal of reactive azo dyes by natural and modified zeolites. *J. Chem. Technol. Biotechnol.* **2003**, *78*, 725–732. [[CrossRef](#)]
54. Mirzaei, N.; Hadi, M.; Gholami, M.; Fard, R.F.; Aminabad, M.S. Sorption of acid dye by surfactant modified natural zeolites. *J. Taiwan Inst. Chem. E.* **2016**, *59*, 186–194. [[CrossRef](#)]
55. Mastropietro, T.F.; Drioli, E.; Candamano, S.; Poerio, T. Crystallization and assembling of FAU nanozeolites on porous ceramic supports for zeolite membrane synthesis. *Microporous Mesoporous Mater.* **2016**, *228*, 141–146. [[CrossRef](#)]
56. Kamboh, M.A.; Solangi, I.B.; Sherazi, S.T.H.; Memon, S. Synthesis and application of p-tert-butylcalix[8]arene immobilized material for the removal of azo dyes. *J. Hazard. Mater.* **2011**, *186*, 651–658. [[CrossRef](#)]
57. Kamboh, M.A.; Solangi, I.B.; Sherazi, S.T.H.; Memon, S. A highly efficient calix[4]arene based resin for the removal of azo dyes. *Desalination* **2011**, *268*, 83–89. [[CrossRef](#)]
58. Kamboh, M.A.; Bhatti, A.A.; Solangi, I.B.; Sherazi, S.T.H.; Memon, S. Adsorption of direct black-38 azo dye on p-tert-butylcalix[6]arene immobilized material. *Arab. J. Chem.* **2014**, *7*, 125–131. [[CrossRef](#)]
59. Kamboh, M.A.; Solangi, I.B.; Sherazi, S.T.H.; Memon, S. Synthesis and application of calix[4]arene based resin for the removal of azo dyes. *J. Hazard. Mater.* **2009**, *172*, 234–239. [[CrossRef](#)]
60. Song, W.; Gao, B.; Xu, X.; Xing, L.; Han, S.; Duan, P.; Song, W.; Jia, R. Adsorption–desorption behavior of magnetic amine/Fe<sub>3</sub>O<sub>4</sub> functionalized biopolymer resin towards anionic dyes from wastewater. *Bioresour. Technol.* **2016**, *210*, 123–130. [[CrossRef](#)]
61. Jin, L.; Sun, Q.; Xu, Q.; Xu, Y. Adsorptive removal of anionic dyes from aqueous solutions using microgel based on nanocellulose and polyvinylamine. *Bioresour. Technol.* **2015**, *197*, 348–355. [[CrossRef](#)]
62. Aliabadi, R.S.; Mahmoodi, N.O. Synthesis and characterization of polypyrrole, polyaniline nanoparticles and their nanocomposite for removal of azo dyes sunset yellow and Congo red. *J. Clean. Prod.* **2018**, *179*, 235–245. [[CrossRef](#)]
63. You, S.J.; Damodar, R.A.; Hou, S.C. Degradation of Reactive Black 5 dye using anaerobic/aerobic membrane bioreactor (MBR) and photochemical membrane reactor. *J. Hazard. Mater.* **2010**, *177*, 1112–1118. [[CrossRef](#)] [[PubMed](#)]
64. Du, W.N.; Chen, S.T. Photo and chemocatalytic oxidation of dyes in water. *J. Environ. Manag.* **2018**, *206*, 507–515. [[CrossRef](#)] [[PubMed](#)]
65. Sala, M.; López-Grimau, V.; Gutiérrez-Bouzán, C. Photo-electrochemical treatment of reactive dyes in wastewater and reuse of the effluent: Method optimization. *Materials* **2014**, *7*, 7349–7365. [[CrossRef](#)] [[PubMed](#)]
66. Sengil, I.A.; Ozacar, M. The decolorization of C.I. Reactive Black 5 in aqueous solution by electrocoagulation using sacrificial iron electrodes. *J. Hazard. Mater.* **2009**, *161*, 1369–1376. [[CrossRef](#)] [[PubMed](#)]
67. Vijayaraghavan, K.; Won, S.W.; Yun, Y.S. Treatment of complex Remazol dye effluent using sawdust and coal based activated carbons. *J. Hazard. Mater.* **2009**, *167*, 790–796. [[CrossRef](#)] [[PubMed](#)]
68. Duman, O.; Tunç, S.; Polat, T.G.; Bozdoğan, B.K. Synthesis of magnetic oxidized multiwalled carbon nanotube r546464-k-carrageenan-Fe<sub>3</sub>O<sub>4</sub> nanocomposite adsorbent and its application in cationic Methylene Blue dye adsorption. *Carbohydr. Polym.* **2016**, *147*, 79–88. [[CrossRef](#)] [[PubMed](#)]
69. Su, Y.; Wu, Z.; Wu, Y.; Yu, J.; Sun, L.; Lin, C. Acid Orange II degradation through a heterogeneous Fenton-like reaction using Fe–TiO<sub>2</sub> nanotube arrays as a photocatalyst. *J. Mater. Chem. A* **2015**, *3*, 8537–8544. [[CrossRef](#)]
70. Sharma, P.; Kaur, H.; Sharma, M.; Sahore, V. A review on applicability of naturally available adsorbents for the removal of hazardous dyes from aqueous waste. *Environ. Monit Assess.* **2011**, *183*, 151–195. [[CrossRef](#)]



71. Lv, J.L.; Zhai, S.R.; Fan, Y.; Lei, Z.M.; An, Q.D. Preparation of  $\beta$ -CD and  $\text{Fe}_3\text{O}_4$  integrated multifunctional bioadsorbent for highly efficient dye removal from water. *J. Taiwan Inst. Chem. Eng.* **2016**, *62*, 209–218. [[CrossRef](#)]
72. Du, K.; Ghorai, U.K.; Chattopadhyay, K.K.; Banerjee, D. Removal of textile dyes by carbon nanotubes: A comparison between adsorption and UV assisted photocatalysis. *Phys. E Low Dimens. Syst. Nanostruct.* **2018**, *99*, 6–15.
73. Cinelli, G.; Cuomo, F.; Ambrosone, L.; Colella, M.; Ceglie, A.; Venditti, F.; Lopez, F. Photocatalytic degradation of a model textile dye using carbon-doped titanium dioxide and visible light. *J. Water Process Eng.* **2017**, *20*, 71–77. [[CrossRef](#)]
74. Hickman, R.; Walker, E.; Chowdhury, S.  $\text{TiO}_2$ -PDMS composite sponge for adsorption and solar mediated photodegradation of dye pollutants. *J. Water Process Eng.* **2018**, *24*, 74–82. [[CrossRef](#)]
75. Copete-Pertuz, L.S.; Pérez-Grisales, M.S.; Castrillón-Tobón, M.; Londoño, G.A.C.; García, G.T.; Martínez, A.L.M. Decolorization of Reactive Black 5 Dye by Heterogeneous Photocatalysis with  $\text{TiO}_2/\text{UV}$ . *Rev. Colomb. Quím.* **2018**, *47*, 36–44.
76. Qiu, M.; Shou, J.; Ren, P.; Jiang, K. A comparative study of the azo dye reactive black 5 degradation by  $\text{UV}/\text{TiO}_2$  and photo-fenton processes. *J. Chem. Pharm. Res.* **2014**, *6*, 2046–2051.
77. Salem, I.A.; El-Ghamry, H.A.; El-Ghobashy, M.A. Catalytic decolorization of Acid blue 29 dye by  $\text{H}_2\text{O}_2$  and a heterogeneous catalyst. *Beni-Suef. Univ. J. Basic Appl. Sci.* **2014**, *3*, 186–192. [[CrossRef](#)]
78. Chen, X.; Wang, W.; Xiao, H.; Hong, C.; Zhu, F.; Yao, Y.; Xue, Z. Accelerated  $\text{TiO}_2$  photocatalytic degradation of Acid Orange 7 under visible light mediated by peroxymonosulfate. *Chem. Eng. J.* **2012**, *193–194*, 290–295. [[CrossRef](#)]
79. Khan, S.R.; Khalid, M.U.; Jamil, S.; Li, S.; Mujahid, A.; Janjua, M.R.S.A. Photocatalytic degradation of reactive black 5 on the surface of tin oxide microrods. *J. Water Health* **2018**, *16*, 773–781. [[CrossRef](#)]
80. Yu, C.H.; Wu, C.H.; Ho, T.H.; Andy Hong, P.K. Decolorization of C.I. Reactive Black 5 in  $\text{UV}/\text{TiO}_2$ ,  $\text{UV}/\text{oxidant}$  and  $\text{UV}/\text{TiO}_2/\text{oxidant}$  systems: A comparative study. *Chem. Eng. J.* **2010**, *158*, 578–583. [[CrossRef](#)]
81. Egerton, T.A.; Purnama, H. Does hydrogen peroxide really accelerate  $\text{TiO}_2$  UV-C photocatalyzed decolouration of azo-dyes such as Reactive Orange 16? *Dye. Pigm.* **2014**, *101*, 280–285. [[CrossRef](#)]
82. Neamtu, M.; Siminiceanu, I.; Yediler, A.; Kettrup, A. Kinetics of decolorization and mineralization of reactive azo dyes in aqueous solution by the  $\text{UV}/\text{H}_2\text{O}_2$  oxidation. *Dye. Pigm.* **2002**, *53*, 93–99. [[CrossRef](#)]
83. Peralta-Zamora, P.; Gouvêa, C.A.K.; Wypych, F.; Durán, N. Effect of  $\text{Na}_2\text{CO}_3$  on the photocatalytic degradation of remazol brilliant blue R. *Toxicol. Environ. Chem.* **2001**, *80*, 83–93. [[CrossRef](#)]
84. Arslan, I.; Balcioglu, I.A. Effect of common reactive dye auxiliaries on the ozonation of dyehouse effluents containing vinylsulphone and aminochlorotriazine dyes. *Desalination* **2000**, *130*, 61–71. [[CrossRef](#)]
85. Wang, Z.; Yuan, R.; Guo, Y.; Xu, L.; Liu, J. Effects of chloride ions on bleaching of azo dyes by  $\text{Co}^{2+}/\text{oxone}$  reagent: Kinetic analysis. *J. Hazard. Mater.* **2011**, *190*, 1083–1087. [[CrossRef](#)] [[PubMed](#)]
86. Molinari, R.; Argurio, P.; Bellardita, M.; Palmisano, L. Photocatalytic Processes in Membrane Reactors. In *Comprehensive Membrane Science and Engineering*, 2nd ed.; Drioli, E., Giorno, L., Fontananova, E., Eds.; Elsevier: Amsterdam, The Netherlands, 2017; pp. 3101–3138.
87. Antoniou, A.I.; Pepe, D.A.; Aiello, D.; Siciliano, C.; Athanassopoulos, C.M. Chemoselective protection of glutathione in the preparation of bioconjugates: The case of trypanothione disulfide. *J. Org. Chem.* **2016**, *81*, 4353–4358. [[CrossRef](#)] [[PubMed](#)]
88. Aiello, D.; Furia, E.; Siciliano, C.; Bongiorno, D.; Napoli, A. Study of the coordination of ortho-tyrosine and trans-4-hydroxyproline with aluminum(III) and iron(III). *J. Mol. Liq.* **2018**, *269*, 387–397. [[CrossRef](#)]
89. Temperini, A.; Piazzolla, F.; Minuti, L.; Curini, M.; Siciliano, C. General, mild, and metal-free synthesis of phenyl selenoesters from anhydrides and their use in peptide synthesis. *J. Org. Chem.* **2017**, *82*, 4588–4603. [[CrossRef](#)] [[PubMed](#)]
90. Minuti, L.; Ballerini, E.; Barattucci, A.; Bonaccorsi, P.M.; Di Gioia, M.L.; Leggio, A.; Siciliano, C.; Temperini, A. A unified strategy for the synthesis of three conical marine natural products. *Tetrahedron* **2015**, *71*, 3253–3262. [[CrossRef](#)]
91. Aiello, D.; Materazzi, S.; Risoluti, R.; Thangavel, H.; Di Donna, L.; Mazzotti, F.; Casadonte, F.; Siciliano, C.; Sindona, G.; Napoli, A. A major allergen in rainbow trout (*Oncorhynchus mykiss*): Complete sequences of parvalbumin by MALDI tandem mass spectrometry. *Mol. Biosyst.* **2015**, *11*, 2373–2382. [[CrossRef](#)]

92. Siciliano, C.; De Marco, R.; Guidi, L.E.; Spinella, M.; Liguori, A. A one-pot procedure for the preparation of N-9-fluorenylmethyloxycarbonyl-  $\alpha$ -amino diazoketones from  $\alpha$ -amino acids. *J. Org. Chem.* **2012**, *77*, 10575–10582. [[CrossRef](#)]
93. Di Donna, L.; Napoli, A.; Sindona, G.; Athanassopoulos, C. A comprehensive evaluation of the kinetic method applied in the determination of the proton affinity of the nucleic acid molecules. *J. Am. Soc. Mass Spectrom.* **2004**, *15*, 1080–1086. [[CrossRef](#)] [[PubMed](#)]
94. Mazzotti, F.; Di Donna, L.; Napoli, A.; Aiello, D.; Siciliano, C.; Athanassopoulos, C.M.; Sindona, G. N-hydroxysuccinimidyl p-methoxybenzoate as suitable derivative reagent for isotopic dilution assay of biogenic amines in food. *J. Mass Spectrom.* **2014**, *49*, 802–810. [[CrossRef](#)] [[PubMed](#)]
95. Ajmal, A.; Majeed, I.; Malik, R.N.; Idriss, H.; Nadeem, M.A. Principles and mechanisms of photocatalytic dye degradation on TiO<sub>2</sub> based photocatalysts: A comparative overview. *Rsc Adv.* **2014**, *4*, 37003–37026. [[CrossRef](#)]
96. Konstantinou, I.K.; Albanis, T.A. TiO<sub>2</sub>-assisted photocatalytic degradation of azo dyes in aqueous solution: Kinetic and mechanistic investigations. A review. *Appl. Catal. B-Environ.* **2004**, *49*, 1–14. [[CrossRef](#)]
97. Saggioro, E.M.; Sousa Oliveira, A.; Pavesi, T.; Maia, C.G.; Vieira Ferreira, L.F.; Costa Moreira, J. Use of titanium dioxide photocatalysis on the remediation of model textile wastewaters containing azo dyes. *Molecules* **2011**, *16*, 10370–10386. [[CrossRef](#)] [[PubMed](#)]



© 2019 by the authors. Licensee MDPI, Basel, Switzerland. This article is an open access article distributed under the terms and conditions of the Creative Commons Attribution (CC BY) license (<http://creativecommons.org/licenses/by/4.0/>).